PHYSICAL REVIEW APPLIED **14,** 031002 (2020)

Letter | Editors' Suggestion

Parity-time Symmetry Based on Time Modulation

Huanan Li,[1,†] Hady Moussa,[1,2,†] Dimitrios Sounas,[3] and Andrea Alù[1,2,4,*]

[1] *Photonics Initiative, Advanced Science Research Center, City University of New York, New York, New York 10031, USA*
[2] *Department of Electrical Engineering, City College of The City University of New York, New York 10031, USA*
[3] *Department of Electrical and Computer Engineering, Wayne State University, Detroit, Michigan 48202, USA*
[4] *Physics Program, Graduate Center, City University of New York, New York, New York 10016, USA*

(Received 19 May 2020; revised 8 July 2020; accepted 23 July 2020; published 11 September 2020)

We leverage aperiodic temporal modulations and nonreciprocity to realize *PT*-symmetric phenomena without the need for gain and loss provided by external mechanisms. We develop our approach using a general coupled-mode framework, and verify our results via detailed simulations in a conservative electronic circuit, demonstrating wave phenomena such as scattering *PT*-phase transition and anisotropic transmission resonances in a Hermitian system. Our concept opens the possibility of implementing *PT*-symmetric phenomena without gain, with applications in sensing, communications, and a broad range of quantum physics.

DOI: 10.1103/PhysRevApplied.14.031002

Introduction—Symmetry plays a central role in our modern understanding of the physical world. Systems respecting the combined parity (P) and time-reversal (T) symmetry have been extensively studied since the work of Bender *et al.*, who proposed a formulation of quantum mechanics based on systems with energy levels all real and positive [1–3]. So far, *PT*-symmetric systems have relied on the delicate balance between gain and loss, which creates fundamental challenges in their actual experimental realization and implementation in quantum settings [4–6]. It is, therefore, not surprising that significant attention on *PT* symmetry has been devoted in the framework of classical physics [7–11], where gain and loss can be controlled, enabling the observation of exciting phenomena like unidirectional invisibility [12,13], sensing enhancement [14–16], laser absorbers [17,18], to name a few. Many of the above functionalities can be traced back to the unique scattering features associated with *PT* symmetry [19,20]. An intriguing question arises on whether we can emulate the response of *PT*-symmetric structures, such as broken *PT*-symmetric phase and unidirectional scattering, in a conservative system, and thus remove the fundamental obstacles, such as gain-induced noise and instabilities, for the experimental investigation of *PT* symmetry in classical and quantum platforms.

Recent attempts to address this challenge have relied on nonlinear phenomena [21] and on time-periodic modulations [22,23], in the context of significant work in the broad area of magnet-free nonreciprocal responses driven by periodic modulations [24–26]. To some extent, both approaches succeed to replace material gain and loss with either wave mixing or parametric oscillations [27]. However, they still heavily rely on some form of external energy and open systems, suffering from instabilities and making it impossible to translate these concepts to quantum settings. In recent years, interesting opportunities have been shown considering slow *nonperiodic modulations in time*, establishing wave phenomena like energy accumulation in lossless structures [28,29] in some ways related to optical trapping enabled by slow light [30], and reconfigurable transport tuning from ballistic to localized [31].

In this paper, we propose a radically different strategy to realize PT-symmetric scattering without gain and loss using aperiodic temporal modulations, inspired by the approach in Ref. [29] to enable energy accumulation in a lossless cavity. Our design for time modulation does not pump energy either in or out of the structure. The generally nonunitary scattering features of *PT* systems are permitted by suitable energy storage and release in the system controlled by nonperiodic time-modulation dynamics. We demonstrate our concept using two coupled resonators under the time-dependent coupled-mode framework. We verify our proposal via detailed numerical simulations, in which we verify the fundamental scattering signatures of *PT*-symmetric systems, including scattering *PT*-symmetric phase transitions and anisotropic transmission resonances (ATR).

*aalu@gc.cuny.edu
†These authors contributed equally.

Modulation-Induced PT-Symmetric Scattering.—We model the time-dependent scattering of wave inputs from two ports $\alpha = L, R$, with flux-normalized amplitudes $s_\alpha^+(t)$, when impinging on our system of two coupled resonators, each supporting a single mode with energy-normalized mode amplitudes ψ_n, $n = 1, 2$. The internal dynamics of the system are dictated by an effective time-dependent Hermitian Hamiltonian $H_0(t) = H_0^+(t)$. We assume that the coupling between the ports and the system, given by a time-dependent real matrix $D(t)$, is reciprocal at each time instant. Correspondingly, the wave output of flux-normalized amplitudes $s_\alpha^-(t)$ can be obtained from the temporal coupled-mode equation [32,33]

$$\begin{aligned} \tfrac{d}{dt}|\Psi\rangle &= [jH_0(t) - \Gamma(t)]|\Psi\rangle + D^T(t)|s^+\rangle, \\ |s^-\rangle &= -|s^+\rangle + D(t)|\Psi\rangle, \end{aligned} \tag{1}$$

where $|s^\pm\rangle = \begin{pmatrix} s_L^\pm \\ s_R^\pm \end{pmatrix}$, $|\Psi\rangle = \begin{pmatrix} \psi_1 \\ \psi_2 \end{pmatrix}$, and $\Gamma(t) = \frac{1}{2}D^+(t)D(t)$, which ensures an (energy) conservative structure. Indeed, we can show from Eq. (1) that

$$\frac{d}{dt}\langle\Psi|\Psi\rangle = \langle s^+|s^+\rangle - \langle s^-|s^-\rangle, \tag{2}$$

ensuring the energy balance within the scatterer and at all ports. In other words, the slow temporal modulation neither injects nor extracts energy into/out of the full setup. Yet, we prove in the following that a suitable nonperiodic modulation of $H_0(t)$ and $D(t)$ can make this conservative system PT symmetric.

To this end, we consider monochromatic wave inputs $s_\alpha^+ \propto e^{j\omega_0 t}$, $\omega_0 \in \mathcal{R}$, and assume for simplicity that $D(t) = \begin{pmatrix} \kappa_+(t) & 0 \\ 0 & \kappa_-(t) \end{pmatrix}$, which means that port L (R) is coupled only with the first (second) resonator via the coupling $\kappa_+(t)$ [$\kappa_-(t)$] [see Fig. 1(a)]. We employ inverse engineering to synthesize a PT-symmetric scattering matrix.

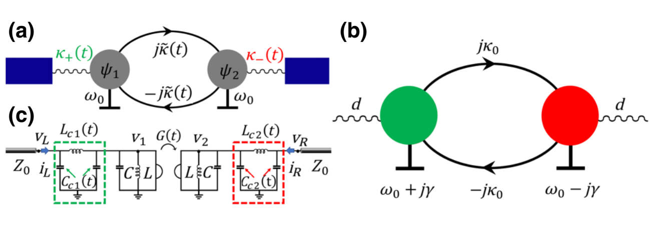

FIG. 1. (a) Schematic of a nonreciprocal coupled-mode system without gain and loss. Slow time modulation in the coupled resonators and in the coupling to the ports enable a PT-symmetric scattering response for monochromatic impinging waves. The response corresponds to the equivalent static PT-symmetric setup (b) with balanced gain ($-j\gamma$) and loss ($j\gamma$). (c) Physical realization of (a) using an electronic lossless circuit with time-dependent gyrator $G(t)$ and two π-networks couplers (within dashed boxes).

Specifically, we set the output $|s^-\rangle = S(\omega_0)|s^+\rangle$ with scattering matrix $S(\omega_0)$ given by

$$S(\omega_0) = -I_2 + jd\frac{1}{h_0 + j\frac{1}{2}d^2 - \omega_0}d, \tag{3}$$

where I_2 denotes the 2×2 identity matrix, the time-independent 2×2 Hamiltonian $h_0 = PTh_0PT$ describes an effective static PT-symmetric target consisting of two coupled single-mode resonators without driving, and the effective time-independent direct coupling between the resonators and their nearby port are equal in strength, and denoted by the parameter d. We define the parity operator $P \equiv \begin{pmatrix} 0 & 1 \\ 1 & 0 \end{pmatrix}$ and T operator to perform complex conjugation.

Generally, we can use our setup Eq. (1) to mimic the PT-symmetric response (3) of an arbitrary Hamiltonian $h_0 = \begin{pmatrix} \omega_0 + j\gamma & \kappa_0^c \\ (\kappa_0^c)^* & \omega_0 - j\gamma \end{pmatrix}$, $\gamma \in \mathcal{R}$, $\kappa_0^c \in \mathcal{C}$. The scattering phenomenon dictated by the effective $S(\omega_0)$ matrix is univocally determined by the two dimensionless parameters $\hat{\gamma} \equiv \gamma/d^2$ and $\hat{\kappa}_0^c \equiv \kappa_0^c/d^2$ [34]. The required time modulation for our structure is found to be [35]

$$H_0(t) = \begin{pmatrix} \omega_0 & \tilde{\kappa}^c(t) \\ [\tilde{\kappa}^c(t)]^* & \omega_0 \end{pmatrix}, \quad \tilde{\kappa}^c(t) = \hat{\kappa}_0^c\, \kappa_+(t)\kappa_-(t) \tag{4}$$

and

$$\kappa_\pm(t) = 1/\sqrt{\kappa_\pm^{-2}(0) \pm 2\hat{\gamma}t} \tag{5}$$

as the driving function for the coupling between the scatterer and the ports. Remarkably, the normalized gain and loss strength $\hat{\gamma}$ for the effective PT-symmetric target is associated with the changing rate of the couplings, although the driving itself does not provide or extract energy, as pointed out above. Physically, effective steady-state dissipation and amplification mechanisms are induced by the temporally varying quality factor of the resonators [35]. As time evolves, Eq. (5) ensures that the coupling between the modes and the connected ports changes in time with the same evolution as the stored energy in the resonators, resulting in "absorption" and "amplification" of the impinging signals from the ports.

The time-dependent coupled mode Eq. (1) are PT symmetric, considering Eqs. (4) and (5) and assuming $\kappa_+(0) = \kappa_-(0)$ for the initial coupling values. Indeed, we can show that $\{|\tilde{s}_-\rangle, |\tilde{s}_+\rangle, |\tilde{\Psi}\rangle\} = PT\{|s_+\rangle, |s_-\rangle, |\Psi\rangle\}$ also satisfy Eq. (1) for any given solution $\{|s_+\rangle, |s_-\rangle, |\Psi\rangle\}$. Notice that in the time domain the T operator sets $t \to -t$ in addition to performing complex conjugation. PT-symmetric scattering manifests itself from the effective PT-symmetric

$S(\omega_0)$ matrix in Eq. (3), which obeys the fundamental relation [19]

$$PTS(\omega_0)PT = S^{-1}(\omega_0). \tag{6}$$

Surprisingly, the PT-symmetric scattering dictated by Eq. (6) does not depend on the initial assumption $\kappa_+(0) = \kappa_-(0)$, see Eq. (3). The generally nonunitary scattering enabled by Eq. (6) originates from Eq. (2). The seeming violation of energy conservation is remedied by the initial conditions of the resonators, and in particular by the stored energy within them at $t = 0$. Indeed, in order to observe the scattering phenomena obeying PT symmetry, the initial state $|\Psi(0)\rangle$ for the system has to be properly prepared: from the second subequation in Eq. (1), we need $|\Psi(0)\rangle = D^{-1}(0)[I_2 + S(\omega_0)]|s^+(0)\rangle$ [35]. In contrast with conventional stationary scattering processes, where the impact of initial states on the scatterer decays exponentially as steady state is reached and thereafter the modes have constant average stored energy, in our scheme the stored energy continuously interplays with the excitation as the resonators change in time and never reach steady state. The initial configuration of few modes correlating with the excitation can be implemented in a reconfigurable way without altering the structure, for instance, by feeding the ports in a short preparation setup before $t = 0$.

Consider the specific scenario when $\kappa_0^c = j\kappa_0$, $\kappa_0 \in \mathcal{R}$, which requires nonreciprocal coupling between the two resonators [see Fig. 1(b)]. This is of special interest because it implements the conditions for PT-symmetric scattering, and nicely connects with the recent interest in the interplay between non-Hermiticity and nonreciprocity [39–41]. From Eq. (4), the required driving for the internal coupling of our system is $\tilde{\kappa}^c(t) = j\tilde{\kappa}(t)$, $\tilde{\kappa}(t) = \hat{\kappa}_0\, \kappa_+(t)\kappa_-(t)$ with $\hat{\kappa}_0 = \kappa_0/d^2$ [see Fig. 1(a)]. This example can be readily implemented in the electronic circuit studied in the following, where the nonreciprocal coupling is provided by a gyrator, see Fig. 1(c) and Ref. [35]. The required initial state $|\Psi(0)\rangle$ is obtained by a preparation signal $|s_+^P(t)\rangle$, $t \le 0$, which, for simplicity, is considered to be monochromatic with frequency ω_0, i.e., $|s_+^P(t)\rangle = e^{j\omega_0 t}|s_+^P(0)\rangle$. We assume that, before time $t = 0$, the driving is absent and the system parameters satisfy $D(t \le 0) = D(0)$ and $H_0(t \le 0) = H_0(0)$. Consequently, associated with an arbitrary input $|s^+(0)\rangle$ for the observation of PT scattering, the amplitudes of the preparation wave $|s_+^P(0)\rangle$ are given by

$$|s_+^P(0)\rangle = \left[I_2 - \frac{\hat{\gamma}}{\hat{\gamma}^2 - \hat{\kappa}_0^2 - 1/4} \times \begin{pmatrix} \hat{\gamma} - 1/2 & \hat{\kappa}_0 \\ \hat{\kappa}_0 & \hat{\gamma} + 1/2 \end{pmatrix}\right] |s^+(0)\rangle. \tag{7}$$

The required initial states $|\Psi(0)\rangle$ depend on the couplings $\kappa_+(0)$ and $\kappa_-(0)$, but interestingly they do not affect the preparation wave $|s_+^P(t)\rangle$, as seen in Eq. (7). This property is also true for the static scattering matrix $S^P(\omega_0)$ in our preparation stage, which is given by

$$S^P(\omega_0) = \begin{pmatrix} -1 + \dfrac{2}{1 + 4\,\hat{\kappa}_0^2} & -\dfrac{4\hat{\kappa}_0}{1 + 4\,\hat{\kappa}_0^2} \\ \dfrac{4\hat{\kappa}_0}{1 + 4\,\hat{\kappa}_0^2} & -1 + \dfrac{2}{1 + 4\,\hat{\kappa}_0^2} \end{pmatrix}. \tag{8}$$

After time $t = 0$, the scattering satisfies PT symmetry for the input $|s^+(t)\rangle = e^{j\omega_0 t}|s^+(0)\rangle$, dictated by the effective PT-symmetric scattering matrix $S(\omega_0)$ in Eq. (3). While in this setup PT symmetry is strictly observed only at the design frequency, it may also be possible to generalize this scheme to operate for a discrete set of frequencies [42].

PT Scattering Using Conservative Circuits.—We validate our analysis considering a lossless circuit implementation. The system is composed of two identical LC resonators, whose complex mode amplitude ψ_n, $n = 1, 2$ in Eq. (1) is defined in terms of the voltage v_n and its derivative with respect to time $\dot{v}_n$ as $\psi_n = \sqrt{C/2}\,[v_n + \dot{v}_n/(j\omega_0)]$, where $\omega_0 = 1/\sqrt{LC}$ is the resonant frequency. The nonreciprocal coupling between the two resonators [see Fig. 1(a)] is implemented by a time-dependent gyrator characterized by conductance $G(t) \equiv \hat{g}(t) \times 2\omega_0 C$. The left and right ports are modeled as two identical transmission lines (TLs) of equal impedance $Z_0 = \hat{r}\sqrt{L/C}$. The port voltages v_α, $\alpha = L, R$ can be decomposed into the

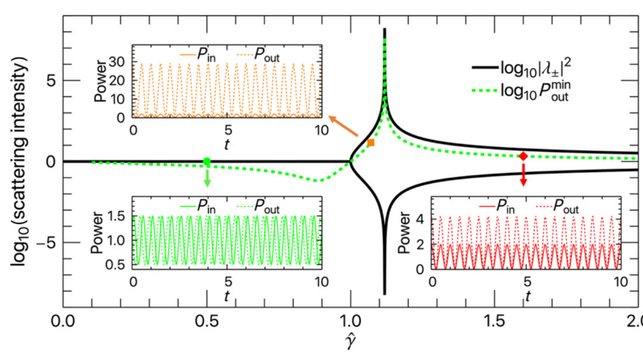

FIG. 2. PT-symmetric phase transition. Semilog plot of the scattering intensity due to $S(\omega_0)$ matrix versus effective gain and loss strength $\hat{\gamma}$ when $\hat{\kappa}_0 = 1$ for the eigenvector inputs $|\lambda_\pm\rangle$ (black solid line) and equal-intensity input $|s_+^{\mathrm{EI}}(t)\rangle \propto \begin{pmatrix} 1 \\ e^{j\phi} \end{pmatrix}$ with $\phi = \phi_{\min}$ (green dashed line). Insets: time-domain simulations for the electronic setup in Fig. 1(c), showing the total power in and out $P_{\mathrm{in/out}}$(W) versus time $t(2\pi/\omega_0)$ after proper initial preparations at $t = 0$, for $\hat{\gamma} = 0.5,\ 1.07,\ 1.6$ (marked by different symbols), and, respectively, for voltage inputs corresponding to equal-intensity input $|s_+^{\mathrm{EI}}(t)\rangle$ with relative phase $\phi = \phi_+,\ \phi_{\min}$, and $\phi_{\min}$. Other parameters are $Z_0 = 50\,\Omega$, $\omega_0 = 2\pi \times 1\,\mathrm{MHz}$ and $\hat{\varepsilon}_1(0) = \hat{\varepsilon}_2(0) = 0.01$, $\hat{r} = 1$, $\phi_0 = -\pi/2$.

input v_α^+ and output v_α^- as $v_\alpha = v_\alpha^+ + v_\alpha^-$, and similarly $i_\alpha = v_\alpha^+/Z_0 - v_\alpha^-/Z_0$ for the port currents i_α. Furthermore, the voltage input and output $v_\alpha^\pm$ is associated with the power wave amplitude $s_\alpha^\pm(t)$ in Eq. (1) via the relation [35]

$$v_\alpha^\pm = \pm j\sqrt{Z_0/2}[s_\alpha^\pm - (s_\alpha^\pm)^*]. \tag{9}$$

We control the coupling between the scatterer and the left and right ports with two π networks $n = 1, 2$, where the inductances $L_{cn}(t) = 1/[\omega_0^2 C_{cn}(t)]$ and capacitances $C_{cn}(t) = [\hat{\varepsilon}_n(t)/\sqrt{\hat{r}}]C$. Figure 1(c) shows a schematic of the electronic setup.

In order to demonstrate PT-symmetric scattering, we consider the proper order of magnitudes $\hat{r} = O(1)$, $\hat{\varepsilon}_n(t) = O(\hat{\varepsilon})$ and $\hat{g}(t) = O(\hat{\varepsilon}^2)$, ensuring weak coupling among resonators and TLs, and employ slow modulation such that the time derivatives $\dot{\hat{\varepsilon}}_n/\omega_0 = O(\hat{\varepsilon}^3)$, $\ddot{\hat{\varepsilon}}_n/\omega_0^2 = O(\hat{\varepsilon}^5)$, and $\dot{\hat{g}}(t)/\omega_0 = O(\hat{\varepsilon}^4)$, etc, where $\hat{\varepsilon} \to 0$ is a small number. Under these assumptions, the coupled-mode model (1) describes our circuit [35] and we can identify the required coupling $\tilde{\kappa}(t) = \omega_0 \hat{g}(t)$ and $\kappa_{+/-}(t) = \sqrt{\omega_0}\hat{\varepsilon}_{1/2}(t)$. The specific driving functions are $\hat{g}(t) = \hat{\kappa}_0 \hat{\varepsilon}_1(t)\hat{\varepsilon}_2(t)$ and $\hat{\varepsilon}_{1/2}(t) = 1/\sqrt{\hat{\varepsilon}_{1/2}(0)^{-2} \pm 2\hat{\gamma}\ \omega_0 t}$. The π-network couplers and gyrator coupling ensure that the resonant frequency ω_0 in Eq. (4) is minimally affected by the surrounding network [29]. We are now ready to illustrate the PT-scattering properties of the circuit. Specifically, we show that our circuit, despite being purely Hermitian, supports a PT-symmetric phase transition and ATR, which follow directly from the fundamental relation Eq. (6) describing a PT-symmetric scattering matrix.

Scattering PT Phase Transition.—Associated with the eigensystem $\{\lambda_\pm, |\lambda_\pm\rangle\}$ of the effective scattering matrix $S(\omega_0)$, i.e., $S(\omega_0)|\lambda_\pm\rangle = \lambda_\pm|\lambda_\pm\rangle$, Eq. (6) indicates that $PT|\lambda_\pm\rangle$ are also its eigenvectors with corresponding eigenvalues $1/\lambda_\pm^*$. The eigenvectors may merge together with their eigenvalues at the exceptional point when $S(\omega_0)$ loses one dimension in its eigenspace. Otherwise, when $PT|\lambda_\pm\rangle \propto |\lambda_\pm\rangle$ yielding $|\lambda_\pm|^2 = 1$, the system supports a symmetric phase. Alternatively, broken-symmetry phase emerges when $PT|\lambda_\pm\rangle \propto |\lambda_\mp\rangle$ and thus $\lambda_\pm = 1/\lambda_\mp^*$. For the circuit, the phase transition can be controlled by tuning $\hat{\gamma}$ for fixed $\hat{\kappa}_0$, as seen observing $\log_{10}|\lambda_\pm|^2$ versus $\hat{\gamma}$ when $\hat{\kappa}_0 = 1$ in Fig. 2. Indeed, we can parametrize the matrix $S(\omega_0)$ in Eq. (3) as

$$S(\omega_0) \equiv \begin{pmatrix} r_L & t_R \\ t_L & r_R \end{pmatrix} = \frac{1}{a}\begin{pmatrix} c & 1 \\ -1 & b \end{pmatrix}, \tag{10}$$

where the real parameters $a = (-1 + 4\hat{\gamma}^2 - 4\hat{\kappa}_0^2)/(4\hat{\kappa}_0)$, $b = \hat{\kappa}_0 + (-1 - 4\hat{\gamma} - 4\hat{\gamma}^2)/(4\hat{\kappa}_0)$ and $bc = a^2 - 1$. An eigenvalue analysis of Eq. (10) shows that symmetry phases emerge when $|\hat{\gamma}/\hat{\kappa}_0| < 1$, while for the broken-symmetric phase, we have $|\hat{\gamma}/\hat{\kappa}_0| > 1$.

The PT-symmetric phase transition can be probed by considering (normalized) equal-intensity inputs $|s_+^{\mathrm{EI}}(t)\rangle = (1/\sqrt{2})\begin{pmatrix} 1 \\ e^{j\phi} \end{pmatrix} e^{j\phi_0} e^{j\omega_0 t}$, where ϕ_0 is an arbitrary initial overall phase [19]. Generally, a broken-symmetry phase leads to amplification of the signal for any relative phase ϕ, namely $P_{\mathrm{out}} = |S(\omega_0)|s_+^{EI}(t)\rangle|^2 > 1$. For the symmetric phase, in contrast, both net amplification and dissipation can arise. Furthermore, when the relative phase ϕ has values $\phi_\pm$ corresponding to the eigenvectors $|\lambda_\pm\rangle \propto \begin{pmatrix} 1 \\ e^{j\phi_\pm} \end{pmatrix}$, we observe a conserved process. In our specific circuit, i.e., $S(\omega_0)$ in Eq. (10), after fixing $\hat{\kappa}_0 = 1$, we obtain the total outgoing power $P_{\mathrm{out}} = (25 - 8\hat{\gamma}^2 + 16\hat{\gamma}^4 + 32\hat{\gamma}\cos\phi)/(5 - 4\hat{\gamma}^2)^2$, which has a minimum value $P_{\mathrm{out}}^{\min}$ for each $\hat{\gamma} > 0$ when the relative phase $\phi = \phi_{\min} = \pi$. In terms of minimum scattering, the circuit experiences dissipation for symmetric phase, while amplification in the broken-symmetric phase, see $\log_{10} P_{\mathrm{out}}^{\min}$ versus $\hat{\gamma}$ in Fig. 2. We emphasize that dissipation and/or amplification in our circuit are due to the energy exchange between signals and the stored energy in the resonators at any instant in time, as the system is still Hermitian and conservative and no energy is provided by or to the modulation network, as shown with a numerical example in Ref. [35]. Given that the system is not time invariant, however, the stored energy in the resonator is not constant at every period, hence resulting in effective dissipation or amplification of the impinging signals.

We perform realistic simulations of the proposed electronic circuit in Fig. 1(c) using Advanced Design System (ADS). In Fig. 2, we show the simulation results for the instantaneous total power in and out of the system $P_{\mathrm{in/out}}(t) = \sum_{\alpha=L,R}[v_\alpha^{+/-}(t)]^2/Z_0$ as a function of time. We consider various sets of parameters $(\hat{\gamma}, \phi) = (0.5, \phi_+)$,$(1.07,\ \phi_{\min})$, and $(1.6, \phi_{\min})$ in both symmetry and broken-symmetry phases, while the other parameters for the simulations are fixed as $Z_0 = 50\,\Omega$, $\omega_0 = 2\pi \times 1\,\mathrm{MHz}$, $\hat{\varepsilon}_1(0) = \hat{\varepsilon}_2(0) = 0.01$, $\phi_0 = -\pi/2$, and $\hat{r} = \hat{\kappa}_0 = 1$. The results match nicely with our CMT prediction Eq. (10), indicated by different symbols in Fig. 2, and the detailed simulation results including scattering in preparation stages before time $t = 0$ are given in Ref. [35].

Nonreciprocal ATR.—Our electronic scattering system involves nonreciprocal coupling between the resonators induced by the gyrator, leading to the response Eq. (3) of effective PT-scattering nature with breaking of left-right transmission symmetry, i.e., $t_L \neq t_R$. Considering $t_L = -t_R = -t \in \mathcal{R}$ in our scenario, Eq. (6) for PT scattering yields the generalized unitarity relation $r_L r_R = 1 - t^2$ and $r_L, r_R \in \mathcal{R}$. Subsequently, in the case the transmittance $T = |t|^2 = 1$, and the reflectance $R_L = |r_L|^2$ or $R_R = |r_R|^2$

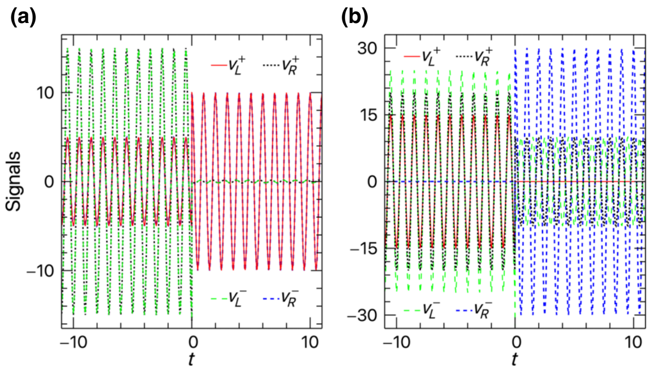

FIG. 3. Demonstration of ATR using the conservative circuit in Fig. 1(c). Input and output voltage signals v_α^+(V) and v_α^-(V) as a function of time $t(2\pi/\omega_0)$ at the port $\alpha = L, R$ when the wave impinges only from the left port (a) and right port (b) after $t = 0$, corresponding respectively to $|s^+(t)\rangle = e^{j\phi_0}e^{j\omega_0 t}\begin{pmatrix}1\\0\end{pmatrix}$ and $e^{j\phi_0}e^{j\omega_0 t}\begin{pmatrix}0\\1\end{pmatrix}$, $t > 0$. In both subfigures, we also show the scattering during the preparation stage $t < 0$. Here $Z_0 = 50\,\Omega$, $\omega_0 = 2\pi \times 1$ MHz, $\hat{\varepsilon}_1(0) = \hat{\varepsilon}_2(0) = 0.01$, $\hat{r} = \hat{\kappa}_0 = 1$, $\phi_0 = -\pi/2$ and $\hat{\gamma} = 3/2$.

vanished, we get a flux-conserving scattering process for a single-side incident wave, which together with $t_L \neq t_R$ leads to nonreciprocal ATR. In our circuit, for example, when $\hat{\gamma} = (1/2)(1 \pm 2\hat{\kappa}_0)$, we have $r_L = 0$, $r_R = -2 \mp (1/\hat{\kappa}_0)$ and $t = \pm 1$ from Eq. (10).

In Fig. 3, we show simulation results for the incoming and outgoing voltage signals when $\hat{\gamma} = 3/2$. As expected, we observe nonreciprocal ATR after time $t = 0$ when the temporal variations turn on. Specifically, in Figs. 3(a) and 3(b), respectively, we get a flux-conserving process $\{v_R^- = v_L^+, v_L^- = 0\}$ for left incidence $\{v_L^+ \neq 0, v_R^+ = 0\}$, and a nonconserving scattering process $\{v_L^- = -v_R^+, v_R^- = 3v_R^+\}$ for right incidence $\{v_L^+ = 0, v_R^+ \neq 0\}$ with very small frequency detuning [35]. In both cases, we also show the scattering response in the corresponding preparation stages when $t < 0$, which precisely matches the theoretical result obtained from Eqs. (7)–(9) [35].

Conclusions.—In this letter, we show that slow aperiodic driving of a coupled resonator system can enable *PT*-symmetric scattering phenomena in purely Hermitian systems, without the need for gain and loss. Nonconservative scattering processes generally expected in *PT*-symmetric systems are allowed by the initial energy stored in the modes. Our study generalizes the concept of *PT* symmetry in time domain to control the release of stored energy in coupled cavities and its interplay with impinging signals to exhibit exotic scattering properties. We implement our proposal in a conservative electronic circuit, and demonstrated phenomena like *PT*-symmetric phase transitions and (nonreciprocal) ATRs. Our approach sheds light on the investigation of *PT*-symmetric systems and may enable their practical implementation in quantum mechanical settings for which Hermiticity is required. Even more opportunities may be offered by considering a larger number of resonant modes, higher dimensions, including synthetic ones, and/or anti-*PT*-symmetry in conservative time-modulated structures.

Acknowledgments.—This work is supported by the Air Force Office of Scientific Research and the Simons Foundation.

[1] C. M. Bender and S. Böttcher, Real Spectra in non-Hermitian Hamiltonians Having PT Symmetry, Phys. Rev. Lett. **80**, 5243 (1998).
[2] C. M. Bender, D. C. Brody, and H. F. Jones, Complex Extension of Quantum Mechanics, Phys. Rev. Lett. **89**, 270401 (2002).
[3] C. M. Bender, Making sense of non-hermitian hamiltonians, Rep. Prog. Phys. **70**, 947 (2007).
[4] H. Schomerus, Quantum Noise and Self-Sustained Radiation of PT-Symmetric Systems, Phys. Rev. Lett. **104**, 233601 (2010).
[5] G. S. Agarwal and K. Qu, Spontaneous generation of photons in transmission of quantum fields in PT-symmetric optical systems, Phys. Rev. A **85**, 031802(R) (2012).
[6] S. Scheel and A. Szameit, PT-symmetric photonic quantum systems with gain and loss do not exist, Europhys. Lett. **122**, 34001 (2018).
[7] L. Feng, R. El-Ganainy, and L. Ge, Non-Hermitian photonics based on parity-time symmetry, Nat. Photonics **11**, 752 (2017).
[8] R. El-Ganainy, K. G. Makris, M. Khajavikhan, Z. H. Musslimani, S. Rotter, and D. N. Christodoulides, Non-Hermitian physics and PT symmetry, Nat. Phys. **14**, 11 (2018).
[9] M.-A. Miri and A. Alù, Exceptional points in optics and photonics, Science **363**, eaar7709 (2019).
[10] S. K. Özdemir, S. Rotter, F. Nori, and L. Yang, "Parity–time symmetry and exceptional points in photonics," Nat. Mater. **18**, 783 (2019).
[11] D. Christodoulides and J. Yang, *Parity-Time Symmetry and Its Applications* (Springer, Berlin, 2018).
[12] Z. Lin, H. Ramezani, T. Eichelkraut, T. Kottos, H. Cao, and D. N. Christodoulides, Unidirectional Invisibility Induced by PT-Symmetric Periodic Structures, Phys. Rev. Lett. **106**, 213901 (2011).
[13] L. Feng, Y.-L. Xu, W. S. Fegadolli, M.-H. Lu, J. E. B. Oliveira, V. R. Almeida, Y.-F. Chen, and A. Scherer, Experimental demonstration of a unidirectional reflectionless parity-time metamaterial at optical frequencies, Nat. Mater. **12**, 108 (2013).
[14] J. Wiersig, Enhancing the Sensitivity of Frequency and Energy Splitting Detection by Using Exceptional Points: Application to Microcavity Sensors for Single-Particle Detection, Phys. Rev. Lett. **112**, 203901 (2014).
[15] W. Chen, S. K. Özdemir, G. Zhao, J. Wiersig, and L. Yang, Exceptional points enhance sensing in an optical microcavity, Nature **548**, 192 (2017).

[16] H. Hodaei, A. U. Hassan, S. Wittek, H. Garcia-Gracia, R. El-Ganainy, D. N. Christodoulides, and M. Khajavikhan, Enhanced sensitivity at higher-order exceptional points, Nature **548**, 187 (2017).

[17] S. Longhi, PT-symmetric laser absorber, Phys. Rev. A **82**, 031801(R) (2010).

[18] Y. Sun, W. Tan, H. Li, J. Li, and H. Chen, Experimental Demonstration of a Coherent Perfect Absorber with PT Phase Transition, Phys. Rev. Lett. **112**, 143903 (2014).

[19] Y. D. Chong, L. Ge, and A. D. Stone, PT-symmetry Breaking and Laser-Absorber Modes in Optical Scattering Systems, Phys. Rev. Lett. **106**, 093902 (2011).

[20] L. Ge, Y. D. Chong, and A. D. Stone, Conservation relations and anisotropic transmission resonances in one-dimensional PT-symmetric photonic heterostructures, Phys. Rev. A **85**, 023802 (2012).

[21] M.-A. Miri and A. Alù, Nonlinearity-induced PT-symmetry without material gain, New J. Phys. **18**, 065001 (2016).

[22] R. El-Ganainy, K. G. Makris, and D. N. Christodoulides, Local PT invariance and supersymmetric parametric oscillators, Phys. Rev. A **86**, 033813 (2012).

[23] T. T. Koutserimpas, A. Alù, and R. Fleury, Parametric amplification and bidirectional invisibility in PT-symmetric time-Floquet systems, Phys. Rev. A **97**, 013839 (2018).

[24] Z. Yu and S. Fan, Complete optical isolation created by indirect interband photonic transitions, Nat. Photonics **3**, 91 (2009).

[25] D. Sounas and A. Alù, Non-Reciprocal photonics based on time modulation, Nat. Photonics **11**, 774 (2017).

[26] I. A. D. Williamson, M. Minkov, A. Dutt, J. Wang, A. Y. Song, and S. Fan, "Breaking reciprocity in integrated photonic devices through dynamic modulation," arXiv:2002.04754.

[27] H. Li, A. Mekawy, and A. Alù, Beyond Chu's Limit with Floquet Impedance Matching, Phys. Rev. Lett. **123**, 164102 (2019).

[28] M. S. Mirmoosa, G. A. Ptitcyn, V. S. Asadchy, and S. A. Tretyakov, Time-Varying Reactive Elements for Extreme Accumulation of Electromagnetic Energy, Phys. Rev. Appl. **11**, 014024 (2019).

[29] D. L. Sounas, Virtual perfect absorption through modulation of the radiative decay rate, Phys. Rev. B **101**, 104303 (2020).

[30] S. Foteinopoulou and J. P. Vigneron, Extended slow-light field enhancement in positive-index/negative-index heterostructures, Phys. Rev. B **88**, 195144 (2013).

[31] H. Li, T. Kottos, and B. Shapiro, Driving-induced metamorphosis of transport in arrays of coupled resonators, Phys. Rev. A **97**, 023846 (2018).

[32] H. A. Haus, *Waves and Fields in Optoelectronics* (Prentice-Hall, Englewood Cliffs, N.J., 1984).

[33] W. Suh, Z. Wang, and S. Fan, Temporal coupled-mode theory and the presence of non-orthogonal modes in lossless multimode cavities, IEEE J. Quantum Electron. **40**, 1511 (2004).

[34] Throughout this paper, variables with hat indicate dimensionless quantities.

[35] See Supplemental Material at http://link.aps.org/supplemental/10.1103/PhysRevApplied.14.031002, which includes Refs. [36–38], for synthesizing *PT*-symmetric scattering in conservative time-modulated systems, the derivation of coupled-mode description of the electronic circuit Fig. 1(c), further simulation results and analysis in the case of equal-intensity inputs $|s_+^{\mathrm{EI}}(t)\rangle$ associated with Fig. 2 and of nonreciprocal ATR associated with Fig. 3.

[36] H. Li, A. Mekawy, A. Krasnok, and A. Alù, Virtual Parity-Time Symmetry, Phys. Rev. Lett. **124**, 193901 (2020).

[37] W. H. Louisell, *Coupled Mode and Parametric Electronics* (John Wiley & Sons, Inc, New York, 1960).

[38] A. H. Nayfeh, *Method of Normal Forms* (Wiley, New York, 1993).

[39] H. Ramezani, Z. Lin, S. Kalish, T. Kottos, V. Kovanis, and I. Vitebskiy, Taming the flow of light via active magneto-optical impurities, Opt. Express **20**, 26200 (2012).

[40] J. M. Lee, S. Factor, Z. Lin, I. Vitebskiy, F. M. Ellis, and T. Kottos, Reconfigurable Directional Lasing Modes in Cavities with Generalized P$\tilde{\mathrm{T}}$ Symmetry, Phys. Rev. Lett. **112**, 253902 (2014).

[41] R. Thomas, H. Li, F. M. Ellis, and T. Kottos, Giant nonreciprocity near exceptional-point degeneracies, Phys. Rev. A **94**, 043829 (2016).

[42] A. A. Zyablovsky, A. P. Vinogradov, A. A. Pukhov, A. V. Dorofeenko, and A. A. Lisyansky, PT-symmetry in optics, Phys.-Uspekhi **57**, 1063 (2014).